Available online at www.sciencedirect.com
SCIENCE DIRECT®
Journal of Chromatography B, 819 (2005) 219–228
JOURNAL OF CHROMATOGRAPHY B
www.elsevier.com/locate/chromb

# Analysis of protein fragmentation inhibition by an MMP-inhibitor in an in vivo model of heart failure using automated chromatography

J. Randall Slemmon [a,*], Cory L. Painter [a,1], Sashi Nadanaciva [a], Florentina Catana [a], Karen Kaup [b,2], Rachel Scherrer [b], Virginia Casadas [b,3], Youyang Zhao [b], Marcia I. Heron [b,3]

[a] *Genomics and Biotechnology, Pfizer Global Research and Development, Skokie, IL 60077, USA*
[b] *Cardiovascular and Metabolic Diseases, Pfizer Global Research and Development, Skokie, IL 60077, USA*

Received 7 May 2004; accepted 6 August 2004
Available online 18 March 2005

**Abstract**

Proteomic strategies have continued to demonstrate value in studying disease by exploiting new technologies that can develop significant numbers of measurements from single samples. However, using complex samples such as tissues or blood has continued to be problematic due to the presence of major interfering substances. In this study, a process is described that uses denaturing peptide extraction from whole tissue and automated chromatography in order to allow subsequent analysis of more than 1000 tissue-derived peptides per sample. The process was employed to identify cardiac proteins that were spared degradation by administration of a heart-protecting matrix metalloproteinase (MMP) inhibitor (compound SC-621) following experimental myocardial infarction (MI). HPLC peptide fingerprints were developed from rat heart left ventricles and the resultant integrated peak data was compared across experimental animals. Surprisingly, although protein fragmentation was generally increased in MI hearts, the effect of the MMP inhibitor was only observed on a few species. The results from this study demonstrated that whole-tissue sample enrichment and peptide analysis using HPLC could be linked in order to study the effects of new compounds on a disease state. The system is flexible and amenable to improvements such as incorporating detection by mass spectrometry.


*Keywords:* Peptides; Proteomics; Biomarkers; Chromatography; SPE; Automation; Heart; Matrix metalloprotease

## 1. Introduction

After organs undergo insult associated with a disease process or an experimental disease model, an array of molecular changes are elicited both within cells and the matrix that surrounds them. Many of these involve the proteolytic breakdown of proteins into peptide fragments. An important example of where such proteolysis is observed is during heart failure [1] and compounds that can impede protein degradation by inhibiting matrix metalloprotease activity, including MMP-13, have been observed to offer protection (e.g. [2,3]). This is likely to become an important avenue for therapy but we are currently hampered by a scarcity of strategies that can discover peptide biomarkers capable of tracking tissue degradation or the effects of experimental drugs that could slow this process.

Proteomic sciences have provided powerful technologies with significant potential for detecting and cataloging large numbers of changes in protein expression. These have included two-dimensional gel electrophoresis coupled to mass-spectrometric identification of the spots (e.g. [4]), single and multi-dimensional liquid chromatography with on-line

* Corresponding author. Present address: Molecular Sciences and Technology, Pfizer Global Research and Development, PGRD 16/345E, 2800 Plymouth Road, Ann Arbor, MI 48105, USA. Tel.: +1 734 622 5969; fax: +1 734 622 1468.
*E-mail address:* Randy.J.Slemmon@Pfizer.com (J.R. Slemmon).
[1] Present address: PGRD 5/136, 2800 Plymouth Road, Ann Arbor, MI 48105, USA.
[2] Present address: Abbott Laboratories, North Chicago, IL 60064, USA.
[3] Present address: Cardiovascular Pharmacology, PGRD, 700 Chesterfield Parkway West, Chesterfield, MO 63017, USA.

1570-0232/$ – see front matter © 2004 Elsevier B.V. All rights reserved.
doi:10.1016/j.jchromb.2004.08.005

analysis by tandem or FTICR mass spectrometry (e.g. [5–8]), and protein reagents such as ICAT (e.g. [9]) or solid-phase isotope tagging [10] that enable mass spectrometric comparisons of protein abundance. However, these techniques are not well positioned for studying changes in hundreds of naturally produced peptides or protein fragments across many samples. Additionally, commercially available mass spectrometric systems are often not well suited to carrying out structural or quantitative analyses on large numbers of unknown protein fragments in real time. Therefore, there is a need for approaches that exploit and integrate additional techniques. In particular, these should include those that are inherently quantitative and yield samples that are amenable to characterization using mass spectrometry either on or off-line. It would also be very useful to develop and characterize more procedures that can efficiently extract peptides from whole tissue in a manner that is quantitative, protects from autolysis during processing and is compatible with high-resolution chromatography and structural analysis.

The study presented here describes a strategy for improving how protein fragments and other naturally occurring peptides can be evaluated as potential biomarkers. It accomplishes this with the aid of an automated chromatographic system that is able to detect changes in protein fragmentation from samples of rat heart. The process first denatures, extracts and enriches tissue peptides and protein fragments away from intact proteins and other tissue contents in a manner that minimizes loss of peptides to precipitates. The captured peptides represent a highly enriched fraction since most of the material from the tissue sample is contained in the protein fraction. The crude peptide material recovered from this process is compatible with multi-dimensional high-resolution automated chromatography and this is employed to further fractionate the peptides. These secondary peptide fractions are then analyzed on reverse-phase HPLC so as to produce peptide profiles showing the prominent peptides and protein fragments extracted from the tissue sample. Exploiting the ease of use and quantitative nature of detection by absorption of ultraviolet light, the relative amounts of the different peptides eluting from HPLC is determined. Grouping of the homologous peptides across HPLC profiles based upon their position in the chromatogram and finding changes that are relevant to the presence of MMP inhibitor across the 30 animals is accomplished with the aid of computer programs that can compare HPLC-generated peptide maps [11]. Peptides showing decreased production in the presence of the MMP-13 inhibitor are characterized.

## 2. Experimental

### 2.1. Matrix metalloprotease inhibitor (MMPi)

The MMP inhibitor (MMPi, SC-621, Pfizer) used in this study is described in International Patent Application WO 00/69821 (23 November 2000, PCT/US00/06719) as example 383 (pages 475, 478 and 535). It has high nanomolar potency against MMP-2 ($IC_{50}$: 700 nM), does not inhibit MMP-1 and inhibits MMP-13 with low nanomolar affinity ($IC_{50}$: 3 nM). Ten milligrams per kilogram of SC-621 was used in this study in order to ensure that plasma drug concentrations were maintained above the $K_i$ for MMP-13 during the dosing interval.

### 2.2. Rat myocardial infarction (MI) model

All studies were conducted with an approved protocol from the Pharmacia Institution for Animal Care and Use Committee (IACUC), and are in accordance with the guidelines set by the Association for the Assessment and Accreditation of Lab Animal Care (AAALAC) for the use of experimental animals. Male Sprague–Dawley rats, weighing 300–350 g, were randomly assigned to one of the following groups: sham-operated (Sham), MI + 0.5% methylcellulose/0.1% Tween-80 (MI + vehicle), or MI + matrix metalloproteinase inhibitor (MI + MMPi). All rats were fasted overnight. On the day of surgery, rats in the MMPi group received their first treatment of compound SC-621 (10 mg/kg, p.o., QD) approximately 4 h prior to surgery, MMPi and vehicle treatments were continued once a day after surgery.

Rats were anaesthetized with isofluorane (4–5%) and intubated. The left side of the thorax was shaved, cleaned with alcohol and scrubbed with betadine. Surgical anesthesia was maintained on all animals with 1–2% isoflurane, with mechanical ventilation. During surgery, all animals were maintained on 1–2% isofluorane surgical anesthesia, and mechanically ventilated. Under sterile conditions, a left thoracotomy was performed to expose the heart. A silk ligature was passed around the left anterior descending artery and for rats in the MI groups, the ligature was tied to permanently occlude the artery, whereas for rats in the sham-operated group the ligature was passed around the artery but not tied. The thorax was closed, muscle layers approximated and sutured, and the skin closed. All rats were given 0.2 mg/kg buprenorphine intramuscularly as a post-operative analgesic, returned to their cages, and allowed to recover. All animals were given food and water ad libitum.

Within each of the groups, euthanasia of cohorts of rats was done on days 3, 7 and 14 post-surgery. At the time of euthanasia, isoflurane provided surgical anesthesia, and entire hearts were removed and quickly rinsed in cold saline. The entire left ventricle free wall including both infarct and peri-infarct tissue was then isolated, rapidly frozen on dry ice, and stored at −80 °C until analysis.

### 2.3. Extraction of peptides from heart tissue and solid phase extraction (SPE)

Rat left ventricle samples had been immediately frozen on dry ice upon harvest and stored at −80 °C. All samples weighed between 450 and 652 mg. Peptides were extracted by homogenizing a frozen sample in 35 ml of 50 mM

sodium phosphate pH 2.5 using a Brinkman Polytron. The homogenate was centrifuged at 48,000 × *g* for 30 min at 15 °C. The supernatant was decanted and held while the pellet was re-homogenized as before in 35 ml of 50 mM sodium phosphate, pH 7.4, containing 750 mM sodium chloride. The re-homogenized sample was centrifuged as before and the supernatant was combined with the previous supernatant. The pellet was discarded. The final pH of the combined supernatants was ca. 2.5. Capture and concentration of the peptides was accomplished using SPE on Waters SepPak cartridges (Environmental, Waters Corp., Milford, MA). Each cartridge was prepared for use by first wetting with 4 ml methanol, washing with 4 ml water and then equilibrating with 4 ml of 0.1% trifluroacetic acid in water. Each supernatant was passed over two SepPak cartridges connected together and placed on the end of a syringe containing the supernatant (Monoject, 140 ml plastic syringe). The tandem cartridges were loaded at a flow rate of 2 ml/min using a Harvard Apparatus syringe pump. The cartridge pairs where then washed with 10 ml of 0.1% trifluoroacetic acid in water and then the cartridges were separated and each one was eluted with 4 ml of wash buffer containing 70% acetonitrile that was collected into 7 ml polypropylene tubes. The samples were dried in a SpeedVac concentrator (ThermoSavant, Hicksville, NY). After drying, the samples were re-suspended in 1.1–1.6 ml of 10 mM sodium phosphate, pH 2.5, containing 10% acetonitrile by using sonication and vortex mixing until the solution appeared clear. The adjustment in volume was carried out in order to normalize all samples based on their original wet weight.

### 2.4. Automated size exclusion/ion exchange separation of captured peptides

The present paradigm exploited the automating abilities of the Applied Biosystems Vision Workstation. A general diagram of the system adapted for this study is shown in Fig. 1, Panel A. Size exclusion was carried out on Sephadex G50 medium (30 cm × 2 cm, Waters AP2 column) in 10 mM sodium phosphate, pH 2.5, containing 10% acetonitrile (Sephadex Buffer) at 2 ml/min. While the sample was developing on Sephadex, specific portions of the elution were captured in series on either reverse-phase or ion

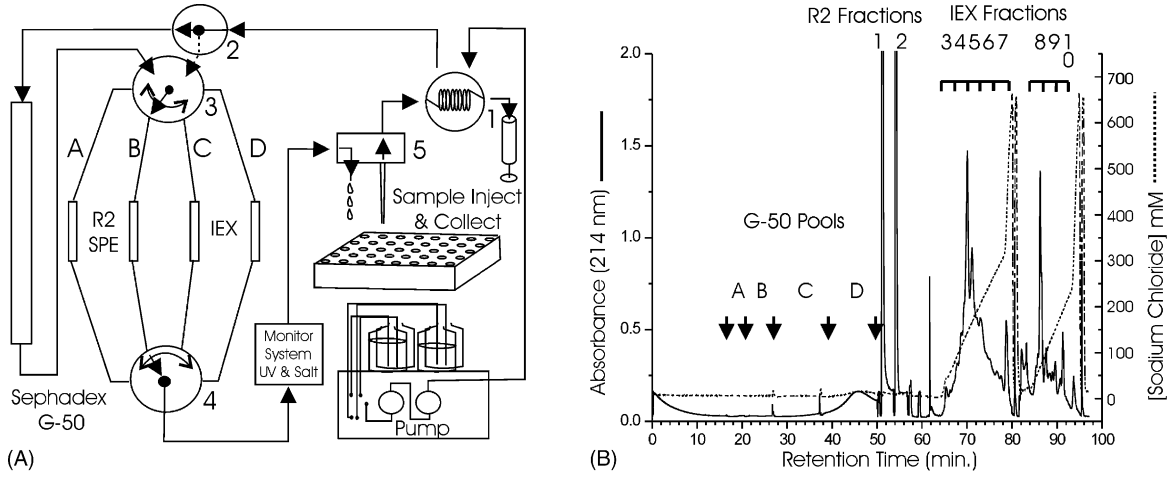


Fig. 1. (A) Configuration employed with the Applied Biosystems Vision Workstation for the fractionation of heart-derived peptides. The Workstation is a self-contained multi-chromatography platform. The final scheme described here reflects a balance between the desire to pre-fractionate heart peptides into a large number of pools and the need to limit the final number of HPLC analyses that must be carried out. Sample injection and collection are handled by the same "Sample Inject & Collect" unit. One milliliter of sample was injected through the injection valve (1) and transferred to the top of the Sephadex G50 medium column (2 cm × 30 cm). Instead of collecting fractions from the Sephadex column, pools were directly captured on secondary columns (A and B, Applied Biosystems Poros R2 reverse-phase, C and D, Amersham Bioscience Source 15S, 0.46 cm × 5 cm) so that further fractionation could be carried out immediately after molecular sizing was complete. At that time, the sizing column is removed from the flow path by rotating valve 2 and then elution is carried out on columns A through D by switching valves 3 and 4 in tandem four times. All columns can be removed from the flow path so that buffer changes within the lines of the instrument can be accomplished quickly using high flow rates that otherwise cause columns to exceed their operating pressure limits. The elution from columns A through D is monitored for conductivity and absorbance of UV light at 214 nm and then collected as fractions in the "Sample Inject & Collect" unit. The four buffers installed on the system are 10 mM sodium phosphate, pH 2.5, containing 10% acetonitrile (size exclusion buffer), 10 mM sodium phosphate, pH 2.7, containing 25% (v/v) acetonitrile (low salt IEX buffer), 10 mM sodium phosphate, pH 2.7, containing 25% (v/v) acetonitrile and 800 mM sodium chloride (high salt IEX buffer) and 0.1% (v/v) trifluoroacetic acid in 70% acetonitrile:29.9% water (R2 hydrophobic elution buffer). The figure represents capabilities of the instrument employed for the current automated separation strategy and does not represent every feature available. (B) Elution data of a representative sample of crude peptides captured from approximately 0.5 g of rat heart left ventricle (operated, 3 days post-operation). In the first 50 min of the program, size exclusion of heart peptides occurs. Pools A through D from size exclusion are captured on columns A through D, respectively, as shown in Panel A. All chromatography is carried out at 2 ml/min. The modest broad peak between 40 and 50 min is principally trifluoroacetic acid salt that carries over with the sample from the initial SPE capture step. After completion of molecular sizing, fractions 1 and 2 are generated by rapid step-elution of all peptides from the Poros reverse-phase (R2) columns, shown as A and B in Panel A. Fractions 3 through 7 are obtained by developing column C (Source 15S Amersham Bioscience, 0.46 cm × 5 cm) in a gradient of sodium chloride buffered in 10 mM sodium phosphate, pH 2.5. Column D is identical to column C and is developed in the same buffer system thereby yielding fractions 8 through 10.

exchange columns. The captured Sephadex pools were labeled A–D (Fig. 1, Panel B) and nominally represented: Pool (A) 30,000 Da and larger, Pool (B) 15,000–30,000 Da, Pool (C) 3,000–15,000 Da and Pool (D) less than 3,000 Da. The larger peptides, represented in Pools A and B, were collected directly onto Poros R2 hydrophobic resin columns (Applied Biosystems, Foster City, CA; prepacked in 0.46 cm × 5 cm Applied Biosystems polymeric columns). Pools C and D, containing the smaller peptides, were captured onto Amersham Bioscience Source15S columns (prepacked in 0.46 cm × 5 cm Applied Biosystems polymeric columns). Both types of column had been pre-equilibrated in Sephadex G50 buffer. At the end of the Sephadex G50 development all columns were placed out of the flow path and the system was flushed at 30 ml/min with 10 volumes of 70% acetonitrile in 0.1% trifluoracetic acid in water. Column A was then placed in line and eluted at 2 ml/min for a total volume of 6 ml. This was collected as a single fraction (fraction 1, Fig. 1, Panel B). Column B was eluted in the same manner and yielded fraction 2. Following this, all columns were again placed off line and the system was flushed with 10 volumes of 10 mM sodium phosphate, pH 2.7, containing 25% (v/v) acetonitrile (low salt buffer). In contrast to the step elution of all peptides from columns A and B, columns C and D were developed in a gradient of sodium chloride. This was accomplished by mixing 10 mM sodium phosphate, pH 2.7, containing 25% (v/v) acetonitrile and 10 mM sodium phosphate, pH 2.7, containing 800 mM sodium chloride. Column C was developed in a 14 ml gradient and collected in five, 2.8 ml fractions (numbers 3–7, Fig. 1, Panel B). After flushing the system in 10 mM sodium phosphate, pH 2.7, containing 25% (v/v) acetonitrile as before, column D was developed in a 12 ml gradient and collected into three, 4 ml fractions (numbers 8–10, Fig. 1, Panel B). Each salt gradient was followed by a 4 ml wash using 10 mM sodium phosphate, pH 2.7, containing 800 mM sodium chloride and was not collected. All fractions were dried in a ThermoSavant SpeedVac vacuum concentrator. The total program time was 97 min per sample and up to 18 samples at one time could be processed on a single instrument in an unattended fashion.

### 2.5. Analysis of peptide pools on HPLC

Fractions 1–10 indicated in Fig. 1, Panel B were analyzed using reverse-phase HPLC. All analyses were carried out on Agilent 1100 HPLC instrumentation consisting of automated sample injection, high-pressure binary gradient formation, column temperature control and UV detection. Dried samples from the Vision Workstation were resuspended in 3.0 ml of 0.1% trifluoroacetic acid in water, of which 1.5 ml was analyzed and the other 1.5 ml was stored frozen at −80 °C. All HPLC employed 0.1% trifluoroacetic acid in water as buffer with acetonitrile as the mobile phase. Reverse phase separation of peptides was carried out on Vydac polymeric C18 columns (0.46 cm × 25 cm, Grace Vydac, Hesperia, CA) at 1 ml/min. The determination of peak retention time (time at peak zenith), peak height and peak area was accomplished with the aid of the Chemstation software that was part of the Agilent HPLC system.

### 2.6. Peak sorting and analysis of HPLC data

All HPLC separations were carried out on peptide recovered from 225 mg of tissue (wet weight). The algorithm for sorting peaks was described previously [11]. All surgeries were carried out on triplicate animal sets so that statistical analysis was carried out with an $n = 3$. Primary interrogation of the data sought significant changes in the level of any peptides between operated animals that had either received inhibitor or vehicle control. This was accomplished using Origin Data Analysis software and a two-population (independent) *t*-test on observations that had been sorted into SAS spreadsheets [11]. *P* values that were less than 0.01 were retained.

### 2.7. Sequencing and mass spectrometry

After determining which peaks had been affected by treatment with compound, the remaining halves of the HPLC samples containing the elevated peptide peaks were combined, concentrated on HPLC and collected. The peak samples were dried in a ThermoSavant SpeedVac and resuspended in 30 ul of 0.1% trifluoroacetic acid. One half of this sample was applied to a Biobrene-treated glass-fiber-filter and 16 cycles of Edman sequencing was carried out in an Applied Biosystems model 490cl pulsed-liquid protein sequencer. The second one-half of the sample was flow injected into a MicroMass LCT mass spectrometer (Waters Corp., Milford, MA) at 20 ul/min that had been configured with a standard electrospray ionization source. Mass determination was carried out using the MaxEnt analysis software (Waters Corp., Milford, MA).

## 3. Results

### 3.1. Extraction of peptides from heart tissue and capture using solid-phase extraction (SPE)

The peptide extraction process used in this study was chosen because it rapidly denatures proteases and other enzymes in the tissue and low pH phosphate buffers were observed to provide for the reproducible extraction of most peptide species. Several reverse-phase SPE materials were evaluated as capture agents for peptides in the initial pH 2.5 supernatant. Those that carry a C18-modified particle and have a pore size that is between 60 and 120 Å show the best performance. Three hundred angstrom or “wide pore” reverse-phase SPE matrices retain considerable protein and this makes dissolving dried samples difficult and often causes loss of peptide to protein precipitates. Additionally, the larger proteins are difficult to recover from ion-exchange chromatography at low pH and they tend to foul columns. The Environmental C18

SepPak from Waters Corp. was chosen because it contains a convenient amount of media in the cartridge (ca. 500 mg) and it is compatible with in-line chromatography due to the presence of Luer fittings on the cartridge. As a result, syringe pumps delivering positive pressure can be used for processing many samples at one time and this can be carried out in an unattended fashion. This greatly facilitates handling the large sample volumes (100 ml) and it prevents gas bubble release from solvents or the need to allow columns to become dry. These are currently problems normally associated with the use of vacuum manifolds for SPE.

### *3.2. Peptide fractionation using automated chromatography and peptide separation on HPLC*

The crude peptide sample recovered from SPE is amenable to processing on commercially available automated chromatography systems. The Vision Workstation (Fig. 1, Panel A) was chosen for this application because it is well suited for tandem chromatography and the control software is well integrated with the hardware. One Vision Workstation is capable of processing a dozen samples a day, which could reasonably support a study containing 50–90 samples in one weeks time. As shown in Fig. 1, Panel B, each 97 min run on the Vision Workstation gives rise to 10 samples for HPLC analysis and each of the resultant HPLC analyses sets requires 900 min. The nearly 1:10 ratio demonstrates that it is the HPLC run time that is rate limiting. However, this is easily balanced by using more than one HPLC instrument. In this study, the 10 groups are analyzed using four identical instruments. Each group is analyzed entirely on one instrument only. In this manner, the HPLC is carried out in less than 10 days thus providing a total turnaround time for the automated chromatography of about 2 weeks. Since much of this is done in an unattended manner, the time frame for the sample analyses is easily accommodated. The process described in this study can define about 1000 peaks per tissue sample based upon absorption of ultraviolet light at 214 nm.

Fig. 2 demonstrates the series of 10 HPLC peptide analyses that are generated from one tissue sample. In preliminary

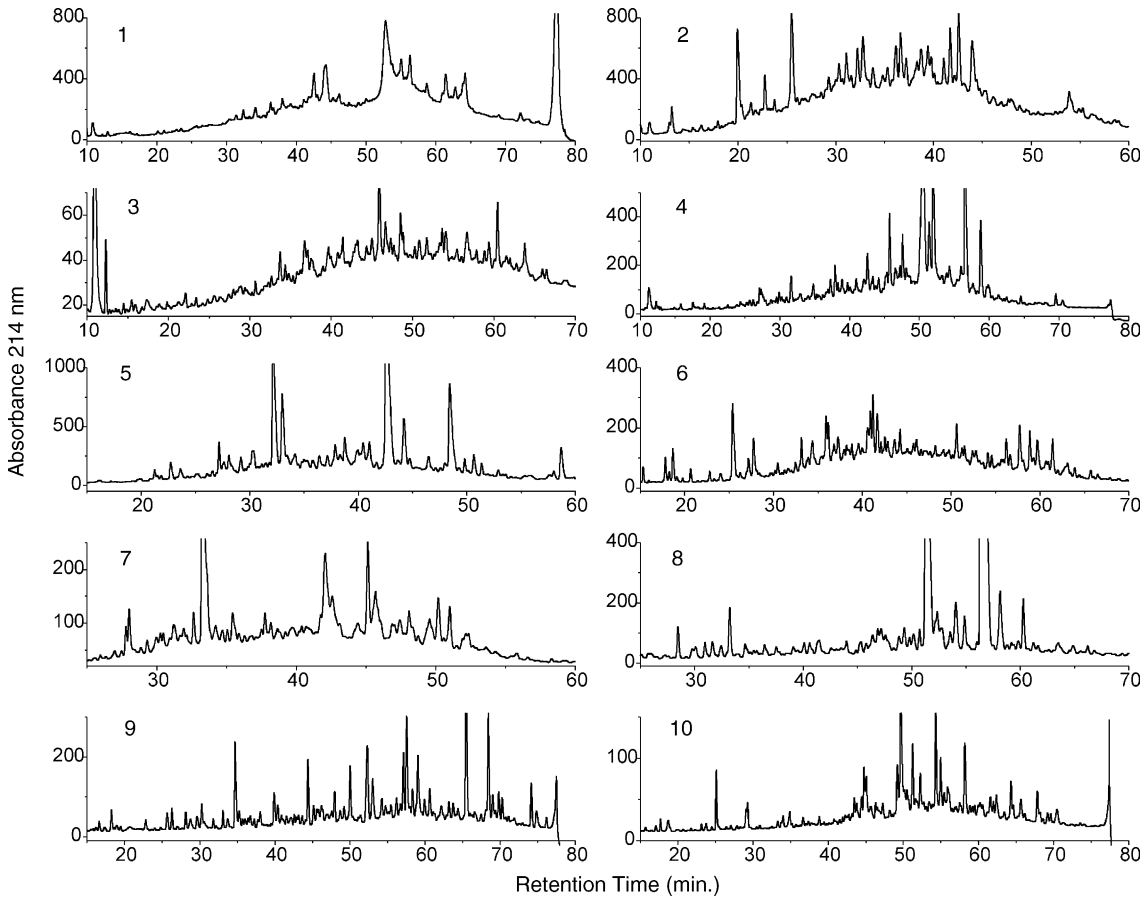


Fig. 2. Representative set of HPLC peptide analyses generated from one rat left ventricle (operated, 3 days post-operation). Panels 1 through 10 represent HPLC separations on peptides from Pools 1 through 10 collected in Fig. 1B. All HPLC analyses used 0.1% trifluoroacetic acid in water as buffer with acetonitrile as the mobile phase. Chromatography is carried out on Vydac polymeric C18 columns (0.46 cm × 25 cm) at 1 ml/min using linear gradients developed over 70 min. Integration of the 214 nm signal nominally yields between 950 and 1000 peaks. Linear gradients are employed and developed as follows. Panels 1 and 2, 20–50% acetonitrile over 80 min. Panel 3, 12–36% acetonitrile over 75 min. Panel 4, 12–40% acetonitrile over 75 min. Panel 5, 14–44% acetonitrile over 65 min. Panel 6, 12–44% acetonitrile over 75 min. Panel 7, 14–48% acetonitrile over 60 min. Panels 8 and 9, 4–34 % acetonitrile over 75 min. Panel 10, 4–36% acetonitrile over 75 min.

studies to determine the best column format to use it was observed that the trade-off between sensitivity and resolution was best met with a 0.46 cm i.d. column. A number of narrower columns were examined, but all failed to offer the necessary peak resolution.

### 3.3. Peak sorting algorithm

Peaking sorting was done with the aid of SAS (Cary, NC) programming language in order to group all peak retention times (and the associated height and peak area information for each peak) into observations. Each observation (line on the spreadsheet) contains the information from the peaks that represent the same peak in each of the 30 chromatograms in an HPLC set (e.g. HPLC of each IEX Fraction 7 from the Vision Workstation, Fig. 1, Panel B). In effect, this produces an electronic overlapping of the 30 HPLC traces obtained from each set of Vision Workstation-derived fractions. This process is then repeated for each of the 10 sets of HPLC traces (see Fig. 2 for an example of one trace from each of the 10 sets) for a final grouping of peak data from 300 HPLC runs. The sorting algorithm accomplishes this within an HPLC set by finding the first peak to elute in any of the 30 HPLC traces in order to begin a new observation. It then looks across the remaining 29 traces for the next earliest peak. It places this next peak into the observation (under its own column) if the earlier peak migrates within 6 s. The newly placed peak in the observation then becomes the reference for the next peak placement. If no more peaks meeting the 6-s criteria are found in subsequent chromatograms, the observation is closed and the next earliest observation from any of the HPLC chromatograms in the set is used to start a new observation. The average retention time for an observation is calculated from the peaks placed in the observation. In this way, finding time windows for peaks is flexible and does not require a beforehand knowledge of peak positions in the HPLC trace.

In a few cases peaks that clearly aligned on the chromatograms are found split between adjacent observations. This can be corrected after evaluating the range in retention times in an observation and combining the observation with the adjacent observation in time if the two observations overlap or are within 6 s. When tight-eluting peak clusters occur within a trace (usually separated by as little as 20 s), they are sorted properly since once an observation is full it is automatically closed. This forces the closely eluting peaks into their own observations. If a peak is below detection on a chromatogram, then it becomes a missing value on the spreadsheet. There are several other properties of the chromatography peaks such as trailing peaks or peak shoulders that can also be used along with elution time in order to identify specific peaks within chromatograms. A more detailed explanation of this can be found in [11].

The properties of a peptide separation from HPLC that allow the algorithm to work effectively are that (1) across a set of elution profiles, all peptides elute nearly the same relative to the other peptides in the same HPLC run, (2) when an HPLC trace in a set of traces shows a shift in the peaks relative to the other traces, the conservation of the position of the peaks relative to one another in a single separation still allows for grouping like-peaks together as long as the traces are not shifted by more than about 40 s, (3) commercially available HPLC columns and instruments deliver highly reproducible peptide separations and (4) the HPLC traces from the same type of sample and from the same fraction of a fractionation scheme are similar. This scheme does not work well on unlike samples such as comparing frog skin extract to bovine heart extract. The spreadsheet approach is amenable to adding mass spectral data to the information about the HPLC peaks. Currently this has been limited primarily by the computer memory required in order to store the spectra from the hundreds of long and complex HPLC separations generated by a single study. The required processing time for MS–MS is also a limitation.

### 3.4. Changes in peaks across animal sets

The entire study includes peptide analysis of 30 left ventricle samples representing naïve and sham-operated hearts along with operated hearts that either did or did not receive inhibitor. Each condition is evaluated after three different time periods post-operation and is carried out on triplicate animals. The data presented is representative of the data set in general and is also chosen to include the only peaks where highly significant changes are captured. Fig. 3, Panels A1–A3, display the peak data integrated by height using the Agilent data analysis software for fraction 6, day 3 post-operation. The general trend for day 3 from all fractions is seen in this figure. Ligated animals receiving inhibitor (A1) and ligated animals that did not (A2) often show elevated peptide levels when compared to the sham-operated control (A3). This demonstrates that protein fragmentation is increased as a result of the ligation and this is due presumably to the activation of several protease activities in the heart.

### 3.5. HPLC peaks that change in the presence of inhibitor to MMP

Fig. 3, Panels B1–B3, shows the analyses of peptides from fraction 6 that represent animals from post-operative day 7. Later-eluting peptides in the ligated animals are still seen as elevated compared to sham-operated animals. However, a few peptides in animals that had been ligated and received inhibitor (B1) are reduced when compared to the parallel animals that did not receive inhibitor (B2). These peptides are noted in Fig. 3, Panel B1 by numbers and arrows. Post-operative day 7 animals are the only ones to show this result and fraction 6 appears to be the only fraction where highly significant changes are apparent. This may be a result of the dose of compound used not being sufficient to affect day 3 post-operative animals due to higher levels of proteolytic activity in these animals.

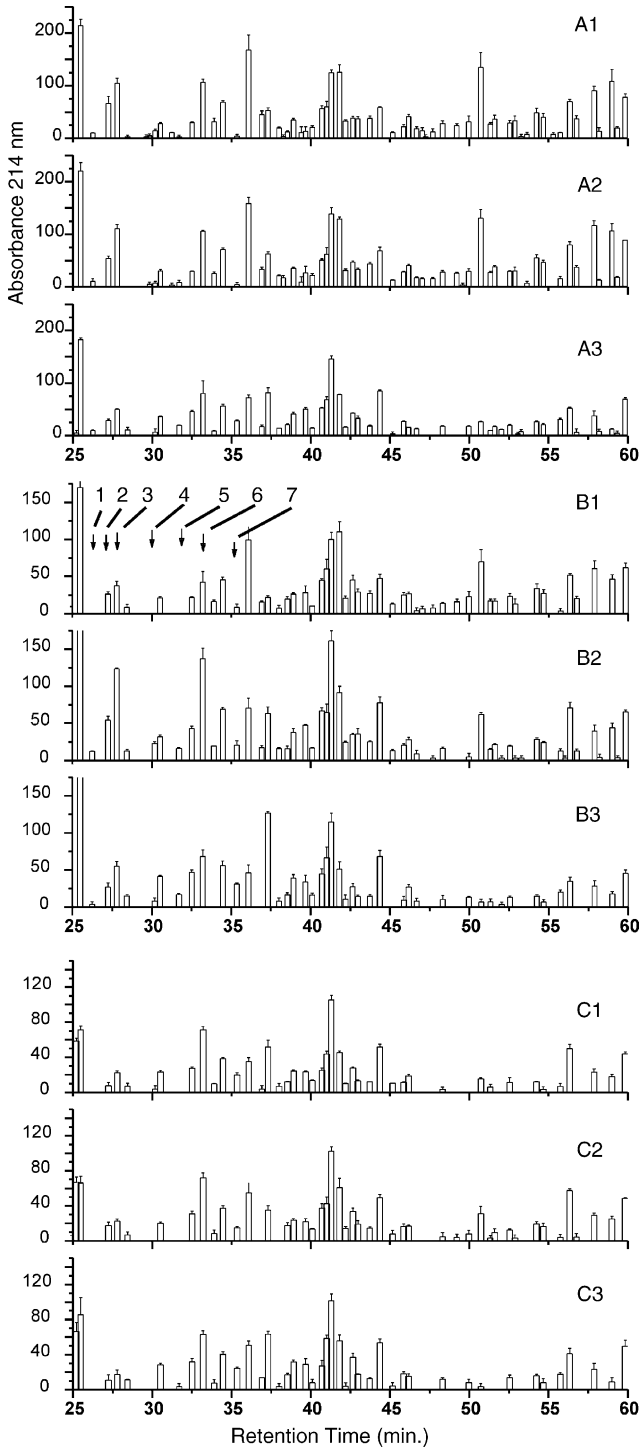


Fig. 3. (A1–A3) Representative peptide analysis data (post-operative day 3, ion-exchange fraction 6). Graphs are generated by sorting HPLC analyses peptide data into spreadsheets based on relative elution time and peak landscape [11]. All error bars are standard error of the mean and are determined from triplicate heart samples. Error reflects both that which is inherent to the analyses as well as from the surgery. (1) Operated animals having received compound. (2) Operated animals not having received compound. (3) Sham-operated animals. (B1–B3) Post-operative day 7, ion-exchange fraction 6. Panels 1–3 correspond to 1–3 in Panel A. Peaks identified as changed in the presence of inhibitor are numbered 1 through 7. (C1–C3) Post-operative day 14, ion-exchange fraction 6. Panels 1–3 correspond to 1–3 in Panel A.

Fig. 3, Panels C1–C3, shows the peptide analyses of the same fraction (Pool 6, Fig. 1, Panel B) but examined 14 days after ligation. Ligated animals (C1 and C2) generated peptide analyses that are more similar to the sham-operated animals (C3), showing that gross proteolysis of the tissue had subsided.

### 3.6. Identification of the peptide(s) from HPLC that were decreased in the presence of inhibitor

The amino terminal sequences and masses of the peptides that change are shown in Table 1 along with the protein that appears as the progenitor of the peptide. They include fragments from cytochrome *C*, actin, hemoglobin and mitochondrial enzymes (Fig. 4). Thymosin beta 4 was recovered intact. The mass accuracy provided by the MicroMass LCT used in this study was maintained within at least 2 Da using Alzheimer's precursor protein fragment 1–40 synthetic peptide as a control. Therefore, the peptides that vary from their expected molecular weight based upon available DNA sequence information reflect either differences between human and rat sequence when rodent DNA sequence is not available, errors in DNA sequence information or post-translational modification of the protein fragment. The amount of peptide

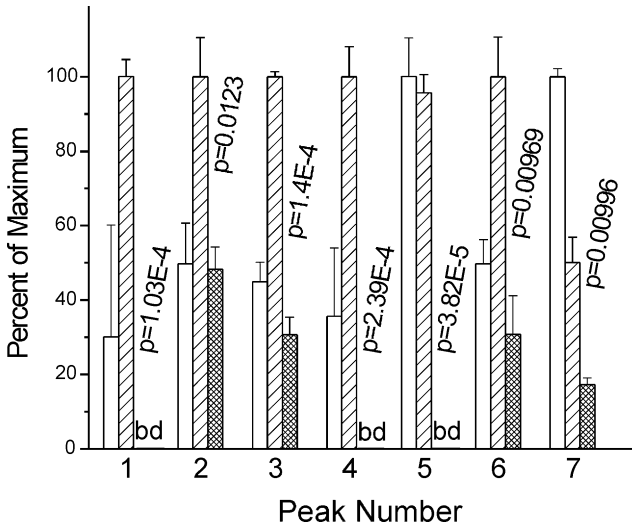


Fig. 4. Relative changes in peptide abundance. Peaks that are altered in operated animals as a result of the inhibitor were identified as discussed in Section 2. Each peptide peak was identified as a fragment of a larger protein, except for thymosin beta 4, which was detected intact. The parent protein corresponding to each peptide peak is: (1) cytochrome *C* reductase binding protein, (2) aortic smooth muscle actin, (3) thymosin beta 4, (4 and 5) alpha hemoglobin, (6) cytochrome *C* oxidase subunit VIa and (7) cytochrome *C* oxidase subunit VIIb. The analyses sought peptides whose abundance is changed between ligated animals that have either received or not received inhibitor. *P* value returns, which triggered identification of the peptide peak, are indicated on the figure over the peak, which is reduced. *P* values were determined by a two-population *t*-test (independent) between control-ligated animals and ligated animals receiving compound. Open bar, sham-operated animals. Single slash bar, ligated animals. Cross-hatched bar, ligated animals that received compound. bd, below detection. Peak numbers 1–7 correspond to peaks 1–7 in Fig. 3, Panel B1.

Table 1
Identification of parent protein from which fragment was derived

| | |
|---|---|
| Peak 1 | |
| Definition | Similar to ubiquinol–cytochrome *C* reductase binding protein; complex III subunit VII [*Mus musculus*, *Rattus norvegicus*] |
| Accession | XP_220421 |
| | IYTWGNQEFAQSK |
| | (50) APPFVLFYLIYTWGNQEFAQSKRKNPA$_{\downarrow}$[1]KYENDK$_{\downarrow}$[2] (82) |
| | 1: 2093 Da expected, 2073 Da measured; 2: 2977 Da expected, 2917 Da measured |
| Peak 2 | |
| Definition | Actin alpha 2, aortic smooth muscle – human |
| Accession | ATHUSM |
| | ISKQEYDEAG |
| | (352) STFQQMWISKQEYDEAGPSIVHRKCF$_{\downarrow}$ (377) |
| | 2207 Da expected for human, 2094 Da measured |
| Peak 3 | |
| Definition | Thymosin beta-4 rat precursor |
| Accession | AAA42246 |
| | SDKPDMAEI |
| | (10) PATMSDKPDMAEIEKFDKSKLKKTETQEKNPLPSKETIEQEKQAGES$_{\downarrow}$ (56) |
| | 4921 Da expected for rat, 4964 Da measured |
| Peak 4 | |
| Definition | Major alpha-hemoglobin rodent |
| Accession | AAA41308 |
| | VLSADDKTNIKNC |
| | (2) VLSADDKTNIKNCWGKIGGHGGEYGEEALQRMF$_{\downarrow}$ (34) |
| | 3625 Da expected, 3606 Da measured |
| Peak 5 | |
| Definition | Major alpha-hemoglobin rodent |
| Accession | AAA41308 |
| | VLSADDKTNIKNC |
| | (2) VLSADDKTNIKNCWGKIGG$_{\downarrow}$ (34) |
| | 2333 Da expected, 2337 Da measured |
| Peak 6 | |
| Definition | Cytochrome *C* oxidase subunit VIa [*R. norvegicus*] |
| Accession | CAA32425 |
| | WLHQGESQRCPNC |
| | (80) ICEEDNCTVIWFWLHQGESQRCPNCGTHYKLVPYQMVH$_{\downarrow}$ (117) |
| | 3112 Da expected, 3112 Da measured |
| Peak 7 | |
| Definition | Cytochrome *C* oxidase subunit VIIb precursor [*Homo sapiens*] |
| Accession | NP_001857 |
| | SHQKKTPTFHDKY |
| | (10) NRLQVRSIQQTMARQSHQKRTPDFHDKYGNAVLASGATFCIVTWTYVATQV$_{\downarrow}$ (80) |
| | 4013 Da expected, 4017 Da measured |

Peptide peaks from HPLC of rat heart protein fragments were analyzed with automated Edman degradation in order to determine the amino terminal sequence and electrospray time-of-flight mass spectrometry in order to estimate the C-terminus. Parent proteins were identified using BLAST database searching for small nearly exact sequences. The best gene definition obtained is given below the peak number. The peptide sequence obtained from Edman degradation is shown over the protein sequence and an estimate of the C-terminus based upon mass data is shown with a down arrow. Numbers in parentheses are the residue numbers from the gene sequence. Measured mass from ES-TOF is indicated, next to the expected mass based upon the gene sequence. Sequences are all indicated with the N-terminus on the left. Details are provided in Section 2.

recovered from most samples was inadequate for completing a comprehensive MS–MS analysis.

## 4. Discussion

In the current study, the proteins represented by the seven peptides whose levels are diminished by the administration of inhibitor fell into three groups. These are hemoglobin, actin and thymosin beta 4 and subunits of mitochondrial enzymes.

### *4.1. Elevation of fragments from hemoglobin in MI*

The elevation of peptides derived from hemoglobin in hearts following myocardial infarction is of considerable interest, especially since it can be inhibited by the administration of compound. The presence of hemoglobin-derived

peptides in tissues is now well documented (e.g. [12] for review) and an elevation in some of these species is observed in Alzheimer's disease brain [13] and models of stroke [14]. Hemoglobin is known to be toxic to tissues (e.g. [15]) and this is likely to occur either through the Fe in the haloprotein (e.g. [16,17]) or the generation of peptides with unexpected bioactivities. The site of proteolysis observed in Peak 4 near residue 34 of alpha hemoglobin could generate a fragment that has been observed to release corticotropin in vitro [18]. Alternatively, the proteolysis of alpha hemoglobin could be part of a process that produces other peptides from the carboxy-terminal region of alpha hemoglobin that potentiate the action of known bioactive peptides such as bradykinin [19]. Consequently, the reduction in hemoglobin fragmentation following MI may be part of the mechanism by which MMP-13-related inhibition protects the heart following MI.

### *4.2. Destruction of thymosin and actin in MI*

The reduction in thymosin beta 4 could work towards the same endpoint as the reduction in actin degradation. Thymosin beta 4 is a widely expressed peptide that is able to bind monomeric actin in a stoichiometric fashion thus preventing polymerization into actin filaments (e.g. for review see [20]). In this manner, it acts as an actin buffer. A decrease in the expression of thymosin beta 4 can therefore be expected to promote cellular repair by promoting actin assembly. In a parallel fashion, the effect of the compound on inhibiting aortic smooth muscle alpha-actin proteolysis will favor this same process by stabilizing the actin pool in cells that express this protein such as the cardiac valve interstitial cells or myofibroblasts (e.g. [21]). Thus, inhibition of MMP-related proteolysis could promote cardiac remodeling by promoting the preservation of cells that support the extracellular scaffolding present in cardiac valves (interstitial cells) or cells involved in wound healing (myofibroblasts).

### *4.3. Degradation of mitochondrial enzyme proteins in MI*

Peaks 1, 6 and 7 were generated from proteins that make up the cytochrome oxidase and reductase complexes found in the mitochondria. Almost 40% of the heart muscle is composed of mitochondria (e.g. [22]) thereby making the fate of the mitochondria a central feature in the fate of the heart. Reduction in the proteolytic degradation of proteins responsible for mitochondrial function such as ATP synthesis may come about in a few ways. First, the compound could decrease protein expression such as is seen in hearts exposed to adriamycin [12]. Secondly, the compound could slow the general destruction of functional mitochondrial proteins that become exposed as a result of mitochondrial swelling (e.g. for review [23]). A consequence of slowing protein degradation under these circumstances may be the inhibition of the release of mitochondrial constituents that are known to induce apoptosis such as cytochrome *C* (e.g. [24]).

## 5. Conclusion

The advent of proteomics has provided rapidly improving technology for the study of proteins and peptides. However, strategies for initially obtaining these from tissues and fluids in a manner that is quantitative, amenable to automation and sufficiently enriched for analytical characterization are improving at a slower rate. The purpose of this study is to establish an automated scheme from commercially available instruments that can exploit the peptide information contained in organs obtained from in vivo studies. To that extent, this scheme works well for viewing more than 1000 peptide peaks per sample and it provides a means for compiling the resultant data into a spreadsheet that allows subsequent interrogation. Although clearly open to more improvements, this study demonstrates that peptide-proteomic strategies offer a useful set of tools for drug discovery.Improvements for the future will include (1) identifying narrow-bore reverse-phase HPLC columns with resolution similar to their wider counterparts and (2) developing detection methods for peptides that are better than traditional in-line ultraviolet absorption (preferably with on-line peptide identification as well).

The ability of this scheme to view changes in protein fragmentation in a more global manner made it ideal for studying the effects of compounds intended to moderate damage to an organ. Additionally, because the markers that are identified are small soluble peptide species it provides candidate biomarkers that may be present in fluids such as blood. Thus, the current strategy offers a means to characterize potential biomarkers at the source of their production and then extrapolate the measurement of these species to blood or urine where they can be studied in a less invasive manner. This strategy can also aid in the identification of in vivo protein substrates for specific proteases and characterize preferred sites of cleavage in vivo. Therefore, taken together the current approach is a significant addition to current proteomic strategies in the discovery of biomarkers.

## References

[1] F.G. Spinale, Circ. Res. 90 (2002) 520.
[2] F.G. Spinale, M.L. Coker, S.R. Krombach, R. Mukherjee, H. Hallak, W.V. Houck, M.J. Clair, S.B. Kribbs, L.L. Johnson, J.T. Peterson, M.R. Zile, Circ. Res. 85 (1999) 364.
[3] H. Li, H. Simon, M.A. Bocan, J.T. Peterson, Cardiovasc. Res. 46 (2000) 298.
[4] W.S. Hancock, S.-L. Wu, P. Shieh, Proteomics 2 (2002) 352.
[5] Y. Shen, R.D. Smith, Electrophoresis 23 (2002) 3106.
[6] D.L. Tabb, M.J. MacCoss, C.C. Wu, S.D. Anderson, J.R. Yates III, Anal. Chem. 75 (2003) 2470.
[7] H. Wang, S. Hanash, J. Chromatogr. B 787 (2003) 11.
[8] M.E. Belov, G.A. Anderson, M.A. Wingerd, H.R. Udseth, K. Tang, D.C. Prior, K.R. Swanson, M.A. Buschbach, E.F. Strittmatter, R.J. Moore, R.D. Smith, J. Am. Soc. Mass Spectrom. 15 (2004) 212.
[9] L-R. Yu, M.D. Johnson, T.P. Conrads, R.D. Smith, R.S. Morrison, T.D. Veenstra, Electrophoresis 23 (2002) 1591.

[10] H. Zhou, J.A. Ranish, J.D. Watts, R. Abersold, Nat. Biotechnol. 19 (2002) 512.
[11] J.R. Slemmon, D.G. Flood, Neurobiol. Aging 13 (1992) 649.
[12] V.T. Ivanov, A.A. Karelin, M.M. Philippova, I.V. Nazimov, V.Z. Pletnev, Biopolymers 43 (1997) 171.
[13] J.R. Slemmon, C.M. Hughes, G.A. Campbell, D.G. Flood, J. Neurosci. 14 (1994) 2225.
[14] T.M. Wengenack, J.R. Slemmon, J.M. Ordy, W.P. Dunlap, P.D. Coleman, Adv. Exp. Med. Biol. 366 (1994) 436.
[15] E.D. Means, D.K. Anderson, J. Neuropathol. Exp. Neurol. 42 (1983) 707.
[16] S.M.H. Sadrzadeh, E. Graf, P.E. Panter, P.E. Hallaway, J.W. Eaton, J. Biol. Chem. 259 (1984) 14354.
[17] I. Yamazaki, L.H. Piette, J. Biol. Chem. 265 (1990) 13589.
[18] A.V. Schally, W.Y. Huang, T.W. Redding, D.H. Coy, K. Chihara, R.C.C. Chang, V. Raymond, F. Labrie, Biochem. Biophys. Res. Commun. 82 (1978) 582.
[19] J.-M. Piot, Q. Zhao, D. Guillochon, G. Ricart, D. Thomas, FEBS Lett. 299 (1992) 75.
[20] T. Huff, C.S.G. Müller, A.M. Otto, R. Netzker, E. Hannappel, Int. J. Biochem. Cell Biol. 33 (2001) 205.
[21] P.M. Taylor, P. Batten, N.J. Brand, P.S. Thomas, M.H. Yacoub, Int. J. Biochem. Cell Biol. 35 (2003) 113.
[22] L.C. Papadopoulou, G. Theophilidis, G.N. Thomopoulos, A.S. Tsiftsoglou, Biochem. Pharmacol. 57 (1999) 481.
[23] J.N. Weiss, P. Korge, H.M. Honda, P. Ping, Circ. Res. 93 (2003) 292.
[24] V. Borutaite, G.C. Brown, FEBS Lett. 541 (2003) 1.